Remote Sens. **2011**, *3*, 1006-1013; doi:10.3390/rs3051006

OPEN ACCESS

Remote Sensing

ISSN 2072-4292

www.mdpi.com/journal/remotesensing

Article

Cloud Remote Sensing Using Midwave IR CO_2 and N_2O Slicing Channels near 4.5 μm

Bo-Cai Gao *, Rong-Rong Li and Eric P. Shettle †

Remote Sensing Division, Code 7230, Naval Research Laboratory, Washington, DC 20375, USA; E-Mail: rong-rong.li@nrl.navy.mil

* Author to whom correspondence should be addressed; E-Mail: gao@nrl.navy.mil; Tel.: +1-202-767-8252; Fax: +1-202-404-8894.

† Retired from Naval Research Laboratory.

Received: 8 April 2011; in revised form: 6 May 2011 / Accepted: 10 May 2011 / Published: 17 May 2011

Abstract: Narrow channels located in the longwave IR CO_2 absorption region between approximately 13.2 and 14.5 μm, the well known CO_2 slicing channels, have been proven to be quite effective for the estimates of cloud heights and effective cloud amounts as well as atmospheric temperature profiles. The designs of some of the near-future multi-channel earth observing satellite sensors cannot accommodate these longwave IR channels. Based on the analysis of the multi-channel imaging data collected with the NASA Moderate Resolution Imaging SpectroRadiometer (MODIS) instrument and on theoretical cloud radiative transfer modeling, we have found that narrow channels located at the midwave IR region between approximately 4.2 and 4.55 μm, where the combined CO_2 and N_2O absorption effects decrease rapidly with increasing wavelength, have similar properties as the longwave IR CO_2 slicing channels. The scattering of solar radiation by clouds on the long wavelength side of the 4.3 μm CO_2 absorption makes only a small contribution to the upwelling radiances. In order to retain the crucial cloud and temperature sensing capabilities, future satellite sensors should consider including midwave IR CO_2 and N_2O slicing channels if the longwave IR channels cannot be implemented on the sensors. The hyperspectral data covering the 3.7–15.5 μm wavelength range and measured with the Infrared Atmospheric Sounding Interferometer (IASI) can be used to further assess the utility of midwave IR channels for satellite remote sensing.

Keywords: remote sensing; cirrus clouds; sensors; spectroscopy; infrared

1. Introduction

The longwave IR CO_2 slicing channels between approximately 13.2 and 14.5 μm have been implemented in a number of meteorological satellite instruments [1,2]. The technique for the retrieval of cloud height and effective cloud amount (the product of cloud fraction and cloud emissivity at 11 μm) has been previously described in detail [3,4]. Multi-years of high cloud statistics obtained from a series of satellite sensors of National Oceanic and Atmospheric Administration (NOAA) have been reported [4]. The CO_2 slicing technique is a well accepted method for inferring cloud height from passive IR remote sensing observations [5].

In spite of the great utility of the longwave IR CO_2 slicing channels for remote sensing of clouds and atmospheric temperature profiles, some of the near-future satellite instruments presently being built will not carry these channels. For example, the VIIRS (Visible/Infrared Radiometer Suite) instruments have selected HgCdTe photovoltaic detectors for the IR focal planes. VIIRS instruments will be flown on the near-future Joint Polar Satellite System (JPSS) mission. The VIIRS IR focal planes cannot accommodate the longwave IR CO_2 slicing channels above 13 μm. The same is true to the SGLI (Second-Generation Global Imager) instrument designed for the future Japanese Global Climate Observation Mission (GCOM). Both VIIRS and SGLI will not have the important cloud and temperature sensing capabilities.

In this article, we report that narrow channels located in the midwave CO_2 and N_2O absorption region near 4.5 μm have similar properties as the longwave IR CO_2 slicing channels based on the analysis of multi-channel imaging data collected with the NASA MODIS instrument [6,7] and on theoretical cloud radiative transfer modeling.

2. The MODIS Instrument Characteristics

MODIS has a total of 36 channels located within a wide spectral range from 0.4 to 14.3 μm. During the early designing phase before 1992, W. P. Menzel proposed to have both the longwave IR CO_2 slicing channels and the midwave IR CO_2 and N_2O slicing channels for MODIS [7]. The wavelength positions and widths of the two sets of channels are listed in Table 1. The four longwave IR CO_2 slicing channels are illustrated in Figure 1(A). The two channels located in stronger gaseous absorption regions at right are most useful for the detection of upper and middle level clouds, while the two channels in weaker gaseous absorption regions at left are affected by radiances from the upper, middle, and lower level clouds as well as surfaces. The three midwave IR channels are illustrated in Figure 1(B). The channel centered at 4.565 μm and marked in a thick broken bar was never implemented on MODIS. This channel was replaced by a channel centered at 1.375 μm for daytime detection of very thin cirrus clouds [8]. The contiguous brightness temperature (BT) curves in Figure 1(A,B) were originated from one spectrum measured above cirrus clouds over the Gulf of Mexico with

the University of Wisconsin High Resolution Interferometer Sounder (HIS) instrument [9] onboard an ER-2 aircraft on December 5, 1991 during a NASA-sponsored cirrus experiment.

Table 1. General characteristics of relevant MODIS midwave and longwave IR channels, including center positions, widths, and saturation brightness temperatures.

Channel	Position (μm)	Width (μm)	Tmax (K)
Longwave IR			
M-33	13.335	0.3	285
M-34	13.635	0.3	268
M-35	13.935	0.3	261
M-36	14.235	0.3	238
Midwave IR			
M-24	4.465	0.05	264
M-25	4.515	0.05	285
-	4.565*	0.05	302

* This channel was originally planned for MODIS, but replaced by a channel centered at 1.375 μm.

Figure 1. Illustration of positions and widths of the MODIS longwave IR CO_2 slicing channels **(A)** and the midwave IR CO_2 and N_2O slicing channels **(B)**. The contiguous curves in (A) and (B) were originated from one HIS spectrum measured above cirrus clouds over the Gulf of Mexico on 5 December 1991 from an ER-2 aircraft at an altitude of 20 km.

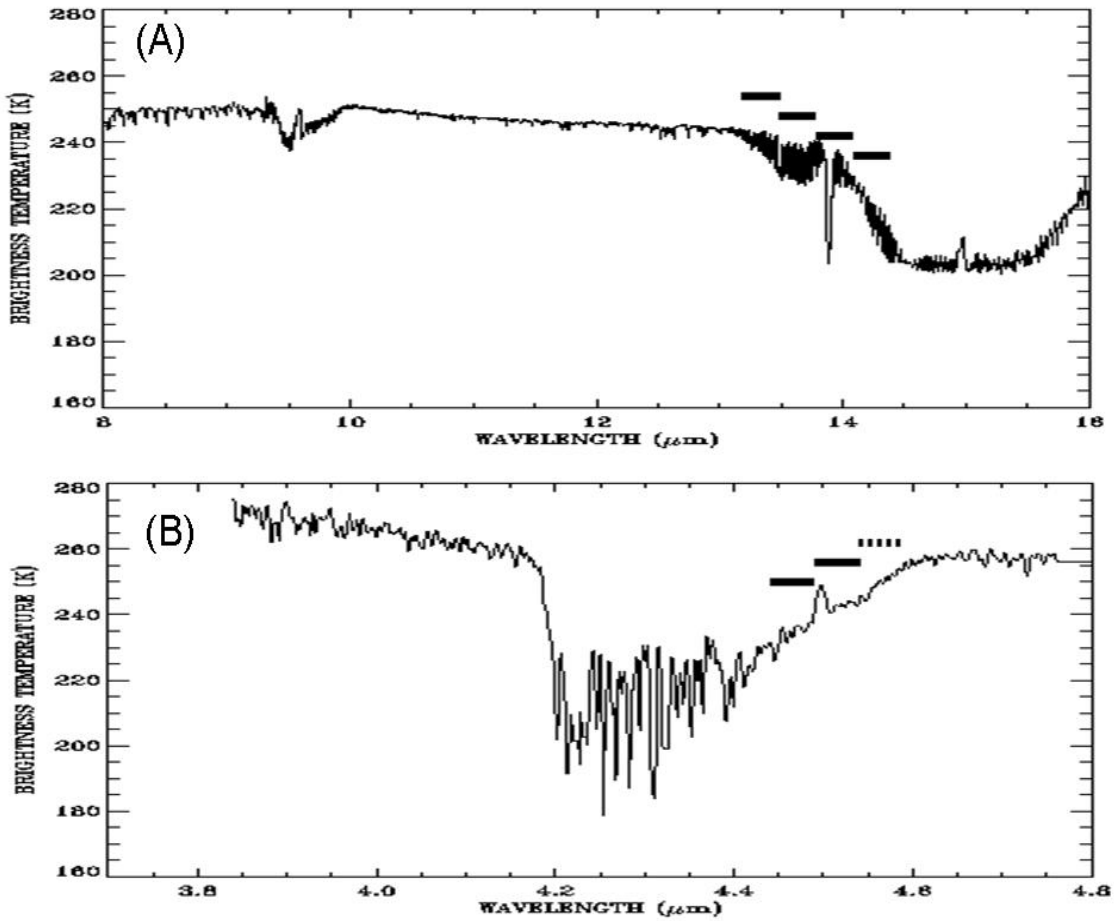

3. Analysis of MODIS Data and Sample Results

We have analyzed a number of MODIS data sets acquired over different geographic regions, in particular the high elevation areas of the Tibet Plateau, the Andes Mountains and Greenland. Very similar results are obtained. The results from the analysis of one data set measured with the Aqua MODIS instrument over the Tibet Plateau and the nearby areas on 21 February 2007 at 0715 UTC are described below.

Figure 2. (A) A color image of processed from 3 images of MODIS channels centered at 0.645 μm (red), 0.55 μm (green) and 0.47 μm (blue), **(B)** the reverse BT image of the midwave IR 4.515-μm channel, and **(C)** the reverse BT image of the longwave IR 13.335-μm channel. See text for detailed descriptions.

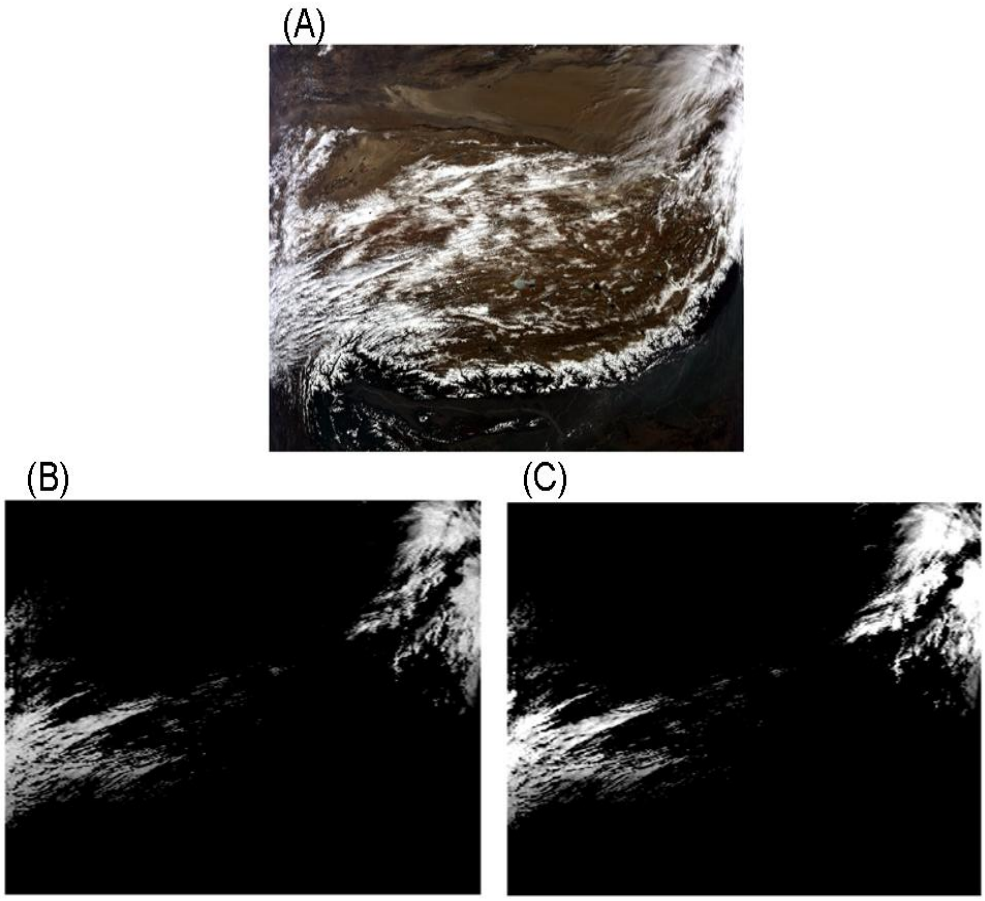

Figure 2(A) shows a "true" color RGB image obtained from the combination of 3 images of MODIS channels centered at 0.645 μm (red), 0.55 μm (green) and 0.47 μm (blue). Clouds and snow over the high elevation Tibet Plateau areas are seen in this image. Figure 3 shows the BT histograms for the four longwave IR channels and the two midwave IR channels. The histogram for the 13.335-μm channel has a peak at approximately 268 K and a long tail below approximately 245 K. The 4.515-μm channel histogram overlaps very well with the 13.335-μm channel histogram, indicating that the two channels have very similar properties in terms of cloud and temperature remote sensing. The histogram of the 13.935-μm channel has almost the same shape as that of the 4.465-μm channel above approximately 230 K. This demonstrates that the two channels have similar properties for atmospheric

remote sensing. Below 230 K, the shapes of the two histograms are different. This is mainly because the detectors used for the 4.465-μm channel lost sensitivity over very cold cloudy pixels. In order to further demonstrate the utility of CO_2 slicing channels for cloud remote sensing, we show in Figure 2(B) the reverse BT image of the 4.515-μm channel, and Figure 2(C) the 13.335-μm channel. When generating the two images, pixels with BT values greater than 240 K were assigned a constant value of zero, and pixels with BT values less than 220 K were assigned a constant value of 255. Pixels with BT values between 220 K and 240 K were assigned values between 0 and 255 based on linear stretching. After such imaging processing, cloudy pixels are selected and clear surface pixels are masked out. The cloud patterns in Figure 2(B,C) are quite similar. This further demonstrated similar properties of the two channels for cloud remote sensing.

Figure 3. The brightness temperature histograms for the 4 longwave IR channels and the two midwave IR channels.

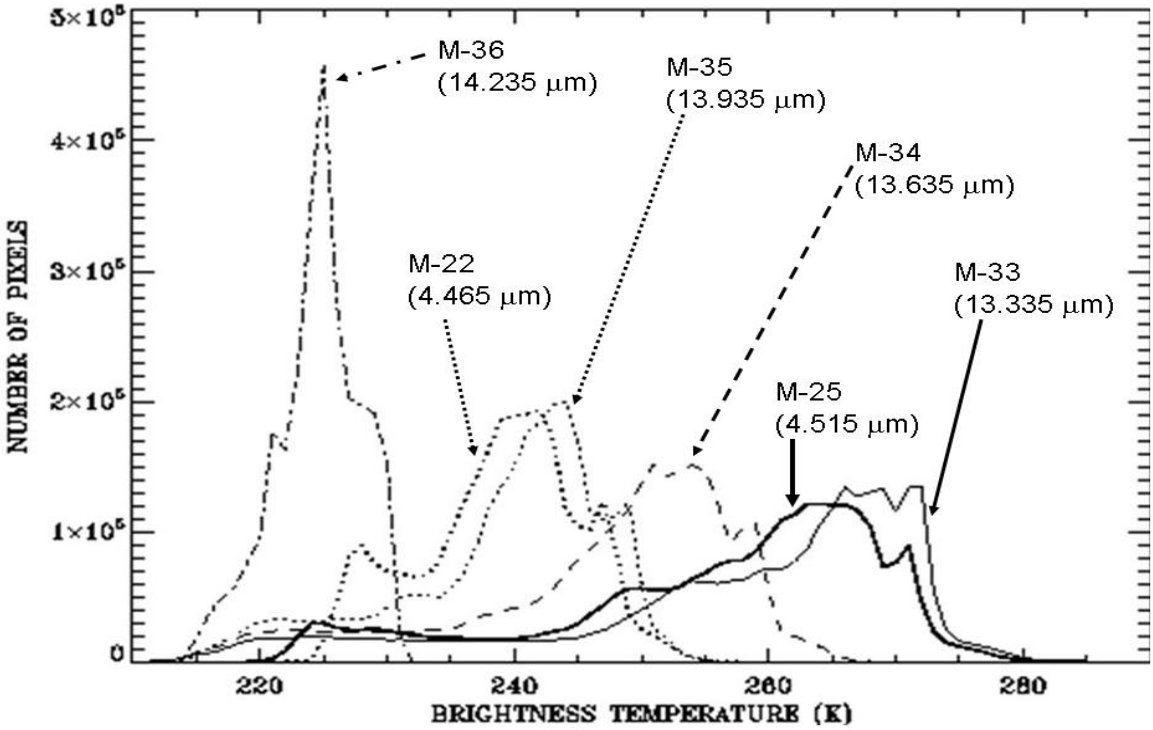

4. Simulation of Ice Cloud Scattering Effects

One concern with the midwave IR CO_2 and N_2O slicing channels is the scattering of solar radiation by ice clouds near 4.5 μm. The cloud scattering effect in the 4-μm atmospheric window region can be seen directly from the Figure 1b spectrum. The BT values generally decrease with increasing wavelength in the 3.85–4.15 μm wavelength range due to decreasing ice particle scattering effects.

In order to have improved understanding of the ice cloud scattering effects, we have made theoretical cloud radiative transfer calculations using the recently available MODTRAN 5 code [10]. A cirrus layer located between 9.3 and 9.8 km with an optical depth of 1 in the visible and an effective spherical ice particle radius of 6 μm (Sub-visual Cirrus) is inserted into the Mid-latitude Summer Model Atmosphere. Radiances and brightness temperatures as a function of wavelength are calculated

separately for two cases—with and without cirrus scattering. Brightness temperature differences between the two cases are also calculated. Similar sets of calculations have been made for the same cirrus layer, but with a much larger effective ice particle radius of 96 μm (Standard Cirrus). Figure 4 shows the BT spectra of a clear atmosphere and the two ice cloud models. The BT differences in the 4.2–4.55 μm atmospheric CO_2 and N_2O absorption region are less than ~1 K. The small BT differences can be attributed to the weak ice particle scattering effects in the wavelength interval and strong atmospheric gaseous CO_2 and N_2O absorption above the cirrus layer. A 1 K warm bias in the apparent cloud top temperature would lead to a less than 200 m altitude reduction in the retrieved cloud height. It should be pointed out that the BT differences in the 3.75–4.15 μm atmospheric window region, and therefore the ice scattering effects, are not negligible, as demonstrated in Figure 4 and Figure 1(B).

Figure 4. Brightness temperature as a function of wavelength. The solid curves correspond to the apparent temperature including solar scattering, and the dashed curves without. Cirrus 1 refers to the MODTRAN Sub-visual cirrus model and Cirrus 2 refers to the Standard Cirrus model. M-24 and M-25 indicate the wavelength range of MODIS Channels 24 and 25. M-Add shows the wavelength coverage of the suggested additional MWIR channel.

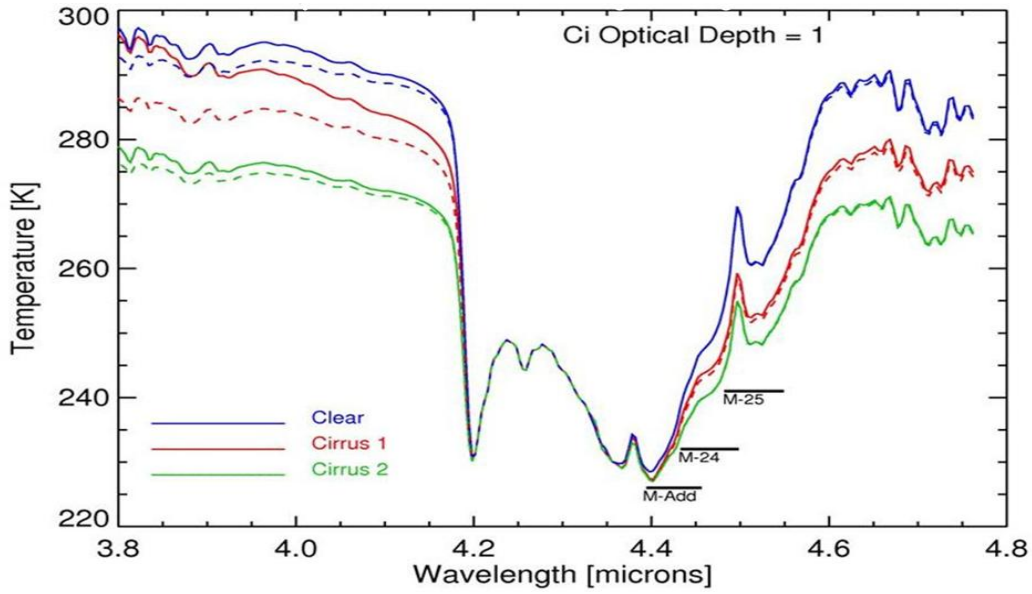

5. Implications on Future Midwave IR CO_2 and N_2O Slicing Channel Selections

In the present MODIS implementation of the midwave IR CO_2 and N_2O slicing channels, the 4.465- and 4.515-μm channels are equivalent to the longwave IR CO_2 13.335- and 13.935-μm channels, respectively. However, a midwave IR channel corresponding to the strong CO_2 absorption channel centered at 14.235 μm is not present. In order to find a midwave IR channel with similar properties as the 14.235-μm channel, we have obtained a mean BT value, $BT_{14.235}$, in the bandpass of the 14.235-μm channel from each of the simulated radiance spectra that correspond to the Figure 4 brightness temperature spectra through box car averaging. Similarly, we have made many box car averaging calculations from these radiance spectra in the midwave IR region with different center wavelength

positions but with a constant width of 0.05 μm. We have found that a channel centered at 4.425 μm with a width of 0.05 μm ("M-Add" in Figure 4) matches the range of $BT_{14.235}$ values. We expect that such a midwave IR channel would have similar properties as the longwave IR 14.235-μm channel in terms of remote sensing of clouds and temperatures. Therefore, we suggest that the 4.425-, 4.465-, 4.515-μm channels can be used as one set of midwave IR channels for reference purposes by future satellite instrument designers. However, the future instrument designers should make more refined specifications for the midwave IR channels based on the analysis of more measured spectral data, such as the HIS data in Figure 1, and more cloud radiative transfer modeling.

6. Conclusions

Based on the analysis of the multi-channel MODIS imaging data and on theoretical cloud radiative transfer modeling, we have found that narrow channels located at the midwave IR region between approximately 4.39 and 4.55 μm, where the combined CO_2 and N_2O absorption effects decrease rapidly with increasing wavelength, have similar properties as the longwave IR CO_2 slicing channels. The scattering of solar radiation by clouds on the long wavelength side of the 4.3 μm CO_2 absorption makes only a small contribution to the upwelling radiances. In order to retain the crucial cloud and temperature sensing capabilities, future studies should consider including midwave IR CO_2 and N_2O slicing channels on satellite sensors if the longwave IR channels cannot be implemented. The hyperspectral data measured with the Infrared Atmospheric Sounding Interferometer and covering the 3.7–15.5 μm spectral range can be used to further assess the utility of midwave IR channels for satellite remote sensing.

Acknowledgements

This research is funded by the NASA MODIS Project and by the Office of Naval Research. We thank S. Ackerman at University of Wisconsin in Madison, Wisconsin for the permission to use the high spectral resolution HIS data.

References

1. Smith, W.L.; Woolf, H.M.; Hayden, C.M.; Wark, D.Q.; McMillin, M. The TIROS-N operational vertical sounder. *Bull. Amer. Meteor. Soc.* **1979**, *60*, 1177-1187.
2. Smith, W.L.; Suomi, V.E.; Menzel, W.P.; Woolf, H.M.; Sromovsky, L.A.; Revercomb, H.E.; Hayden, C.M.; Erickson, D.N.; Mosher, F.R. First sounding results from VAS-D. *Bull. Amer. Meteor. Soc.* **1981**, *62*, 232-236.
3. Menzel, W.P.; Smith, W.L.; Stewart, T.R. Improved cloud motion wind vector and altitude assignment using VAS. *J. Appl. Meteor.* **1983**, *22*, 377-384.
4. Wylie, D.P.; Menzel, W.P. Eight years of high cloud statistics using HIRS. *J. Climate* **1999**, *12*, 170-184.
5. Smith, W.L.; Frey, R. On cloud altitude determinations from high resolution interferometer sounder (HIS) observations. *J. Appl. Meteor*. **1990**, *29*, 658-662.

6. Salomonson, V.V.; Barnes, W.L.; Maymon, P.W.; Montgomery, H.E.; Ostrow, H. MODIS: Advanced facility instrument for studies of the earth as a system. *IEEE Trans. Geosci. Remote Sens.* **1989**, *27*, 145-153.
7. King, M.D.; Kaufman, Y.J.; Menzel, W.P.; Tanre, D. Remote sensing of cloud, aerosol and water vapor properties from the Moderate Resolution Imaging Spectrometer (MODIS). *IEEE Trans. Geosci. Remote Sens.* **1992**, *30*, 2-27.
8. Gao, B.-C.; Kaufman, Y.J. Selection of the 1.375-μm MODIS channel for remote sensing of cirrus clouds and stratospheric aerosols from space. *J. Atmos. Sci.* **1995**, *52*, 4231-4237.
9. Revercomb, H.E.; Buijs, H.; Howell, H.B.; LaPorte, D.D.; Smith, W.L.; Sromovsky, L.A. Radiometric calibration of IR Fourier transform spectrometers: Solution to a problem with the High-resolution Interferometer Sounder (HIS). *Appl. Opt*. **1987**, *27*, 3210-3218.
10. Berk, A.; Anderson, G.P.; Acharya, P.K, Bernstein, L.S.; Muratov, L.; Lee, J.; Fox, M.; Adler-Golden, S.M.; Chetwynd, J.H.; Hoke, M.L.; Lockwood, R.B.; Gardner, J.A.; Cooley, T.W.; Borel, C.C.; Lewis, P.E.; Shettle, E.P. MODTRAN™ 5: 2006 Update. *Proc. SPIE* **2006**, *6233*, 62331F.